Three-Phase Power Flow Based on Four-Conductor Current Injection Method for Unbalanced Distribution Networks

Debora Rosana Ribeiro Penido, *Student Member, IEEE*, Leandro Ramos de Araujo, Sandoval Carneiro, Jr., *Senior Member, IEEE*, Jose Luiz Rezende Pereira, *Senior Member, IEEE*, and Paulo Augusto Nepomuceno Garcia, *Member, IEEE*

***Abstract*—This work presents a new formulation for the power flow problem, with explicit representation of the neutral conductor and grounding. This methodology has been named the four-conductor current injection method (FCIM). The Newton–Raphson method is applied to solve the set of nonlinear current injection equations that are derived using phase coordinates, and the complex variables are written in rectangular form. The proposed algorithm can be used to analyze both balanced and unbalanced systems, meshed or radial, with controls and distributed generation, and is shown to be very efficient and robust for large scale systems.**

***Index Terms*—Current injection method, distributed generation, distribution systems, four-wire systems, induction machine modeling, three-phase power flow, unbalanced operation.**

I. Introduction

ELECTRICAL distribution systems (DS) are expected to experiment considerable growth in the near future, with respect to the penetration of distributed generation (DG). This will be mainly due to several factors, ranging from environmental concerns to new technologies such as fuel cells and other alternative energy sources. In spite of the additional complexity in DS planning and operation in the presence of DG, it is of paramount importance that the performance of these systems should be continuously improved to ensure increasing levels of power quality to the customers. This will be achieved mainly through new operational procedures, technological developments and advanced analytical tools. New load-flow programs and new algorithms based on optimization methods are being developed to assist engineers in all matters related to the expansion and operation planning of DS.

It is well-known that most DS are considerably unbalanced, and in high density load areas such as city centers, the network topology can be highly meshed. Under these circumstances, the three-phase four-conductor configuration with multiple neutral grounding has been largely adopted, due to smaller installation costs and better sensitivities for fault protection, when compared with the three-phase three-conductor configuration. The presence of neutral conductors and grounding affect not only the system operation but also equipment and human safety [1].

Several methodologies have been proposed to solve the power flow problem in three-phase DS [2]–[11]. The forward-backward sweep (FBS) has been preferred by many authors, due to its good performance and simplicity of implementation. However, FBS may require a large number of iterations for heavy-load conditions and especially when control devices and DG are present in the system. It also presents limitations to solve non-radial (meshed) DS. Additional features have been incorporated in some FBS algorithms to overcome such difficulties [10]–[14] but in some cases the computational effort has increased considerably, and convergence is not achieved in some cases [16].

In recent years the three-phase current injection method (TCIM) has been proposed [7]. TCIM is based on the current injection equations written in rectangular coordinates and is a full Newton method. As such, it presents quadratic convergence properties and convergence is obtained for all but some extremely ill-conditioned cases. Further TCIM developments led to the representation of control devices [8], [9]. New very efficient routines have been developed to perform matrix ordering and factorization [15] and thus TCIM has become competitive with FBS for purely radial systems and appears to be more robust computationally for meshed DS, as well as in the presence of control devices [16]. However TCIM does not allow for the representation of grounding and neutral conductors.

The four-conductor current injection method (FCIM) was conceived to include the explicit representation of neutral conductors and grounding. In [17] the basic equations were presented and a simple test system was used to illustrate the proposed methodology. Work on the method progressed with the inclusion of improved component models and the development of new models for transformers, voltage regulators and induction machines.

The present paper revises the equations derived in [17], and describes some of the latest developments including the representation of PV nodes and DG. The PV node model was extended to include the neutral connection, which can be isolated, solid-grounded or grounded through impedance. An induction machine model including some control strategies

Manuscript received November 29, 2006; revised September 17, 2007. This work was supported in part by the National Research Council, CNPq. Paper no. TPWRS-00848-2006.

D. R. R. Penido is with the Eletrobras, Rio de Janeiro, RJ, Brazil (e-mail: debora@eletrobras.com).

L. R. de Araujo is with the Petrobras, Rio de Janeiro, RJ, Brazil (e-mail: leandroaraujo@petrobras.com.br).

S. Carneiro, Jr is with the Department of Electrical Engineering, COPPE, Federal University of Rio de Janeiro, Rio de Janeiro, RJ, Brazil (e-mail: sandoval@coep.ufrj.br).

J. L. R. Pereira and P. A. N. Garcia are with the Department of Electrical Engineering, Federal University of Juiz de Fora, Juiz de Fora, MG, Brazil (e-mail: jluiz@ieee.org; pgarcia@lacee.ufjf.br).

Color versions of one or more of the figures in this paper are available online at http://ieeexplore.ieee.org.

Digital Object Identifier 10.1109/TPWRS.2008.919423

was created to represent the presence of DG [22], [23]. The methodology was implemented in C++ using object-oriented programming techniques to attain improved flexibility, computational performance and modularity. The proposed approach is validated using several test cases including a large-scale practical DS.

II. Formulation of FCIM

A. Review of the Basic Equations

The proposed four-conductor power flow formulation is based on the current injected at every node of the power system, expressed in terms of series and shunt connections.

The current injection contribution for series components is given by

$$I^s_{k,series} = \sum_{i\in\Omega_k}\sum_{t\in\alpha_p}\left(jb^{st}_{ki_{sh}}V^t_k + \left(V^t_k - V^t_i\right)y^{st}_{ki}\right) \quad (1)$$

where

V^t_k phase t to ground voltage phasor at bus k;

V^t_i phase t to ground voltage phasor at bus i;

shunt suscepttance of element $k-i$;

$b^{st}_{ki_{sh}}$ when $s=t$, then it is the self susceptance of phase s or when $s\neq t$ then it is the mutual susceptance between phases s and t;

$s,t\in\alpha_p$ $\alpha_p=\{a,b,c,n\}$;

Ω_k set of buses directly connected to bus k;

series admittance of element $k-i$;

y^{st}_{ki} when $s=t$, then it is the self admittance of phase s or when $s\neq t$ then it is the mutual admittance between phases s and t.

It is seen that the terms in (1) allow for mutual couplings in the components. The lines model is based on [25].

The current injection contribution of a shunt component depends on the kind of connection and model adopted. For components modeled as phase admittances in wye connection with the neutral grounded through admittance, the current contribution is given by

$$I^n_{k,sh} = y^n_{k_{gr}}V^n_k + \sum_{d\in\alpha_d} y^d_k\left(V^n_k - V^d_k\right) \quad (2)$$

$$I^d_{k,sh} = y^d_k\left(V^d_k - V^n_k\right) \quad (3)$$

where

$d\in\alpha_d$ $\alpha_d=\{a,b,c\}$;

V^d_k phase d to ground voltage phasor at bus k;

V^n_k Neutral to ground voltage phasor at bus k;

y^d_k admittance between phase d and neutral at bus k;

$y^n_{k_{gr}}$ neutral grounding admittance at bus k.

For components modeled as phase admittances directly connected to ground the current injection contribution can be expressed as

$$I^s_{k,sh} = y^s_{k_{sh}}V^s_k \quad (4)$$

where $y^s_{k_{sh}}$ is the s node grounding admittance at bus k.

Thus the total current injected at phase s of bus k is given by

$$I^s_k = I^s_{k,sh} + I^s_{k,series}. \quad (5)$$

This net current injected at phase s of bus k can be expressed in terms of the nodal admittance matrix as

$$I^s_k = \sum_{t\in\alpha_p} Y^{st}_{kk}V^t_k + \sum_{\substack{i\in\Omega_k\\ i\neq k}}\sum_{t\in\alpha_p} Y^{st}_{ki}V^t_i \quad (6)$$

where $Y_{kk} = G_{kk} + jB_{kk}$ and $Y_{ki} = G_{ki} + jB_{ki}$ are the elements of the nodal admittance matrix.

Generation units and loads are normally specified for power flow studies as net injected complex powers, in which case the equation for grounded-wye connection is given by

$$S^d_k = P^d_k + jQ^d_k = \left(V^d_k - V^n_k\right)I^{d}_{k,\mathrm{lg}}{}^{*}. \quad (7)$$

Thus the current injection contribution by loads and generators, for phases a, b and c, can be expressed as

$$I^d_{k,\mathrm{lg}} = \frac{\left(P^d_k - jQ^d_k\right)}{\left[\left(V^d_{\mathrm{Re}_k} - V^n_{\mathrm{Re}_k}\right) - j\left(V^d_{\mathrm{Im}_k} - V^n_{\mathrm{Im}_k}\right)\right]}. \quad (8)$$

The neutral current injection contribution is given by

$$I^n_{k,\mathrm{lg}} = -\left(I^a_{k,\mathrm{lg}} + I^b_{k,\mathrm{lg}} + I^c_{k,\mathrm{lg}}\right). \quad (9)$$

The net specified complex power is a function of the generation and load, as (10) and (11)

$$P^d_k = P^d_{G_k} - P^d_{D_k} \quad (10)$$

$$Q^d_k = Q^d_{G_k} - Q^d_{D_k} \quad (11)$$

where, at bus k

S^d_k specified net injected complex power in phase d;

P^d_k, Q^d_k specified net active and reactive powers in phase d;

$I^d_{k,\mathrm{lg}}$ phase d current injection, contribution of a load or generation unit;

$P^d_{G_k}, Q^d_{G_k}$ active and reactive power generation in phase d;

$P^d_{D_k}, Q^d_{D_k}$ active and reactive power demand in phase d;

$V^d_k = V^d_{\mathrm{Re}_k} + jV^d_{\mathrm{Im}_k}$ phase d to ground voltage phasor;

$I^d_k = I^d_{\mathrm{Re}_k} + jI^d_{\mathrm{Im}_k}$ phase d current injection at bus k.

The well-known composite ZIP load model for wye connection can be written as

$$P_k^d = P_{G_k}^d - \left(P_{P_k}^d + P_{I_k}^d \left|V_k^d - V_k^n\right| + P_{Z_k}^d \left|V_k^d - V_k^n\right|^2\right) \quad (12)$$

$$Q_k^d = Q_{G_k}^d - \left(Q_{P_k}^d + Q_{I_k}^d \left|V_k^d - V_k^n\right| + Q_{Z_k}^d \left|V_k^d - V_k^n\right|^2\right) \quad (13)$$

where $|V_k^d - V_k^n|$ is the magnitude of the phasor difference between the phase d to ground voltage and the neutral to ground voltage at bus k, and $P_{P_k}^d, P_{I_k}^d, P_{Z_k}^d, Q_{P_k}^d, Q_{I_k}^d, Q_{Z_k}^d$ are the active and reactive power parts of ZIP model.

The following relations are defined to simplify the derivations of the Jacobian:

$$P_k'^d = P_{G_k}^d - P_{P_k}^d \quad (14)$$

$$Q_k'^d = Q_{G_k}^d - Q_{P_k}^d. \quad (15)$$

Equations (6), (8) and (9) are combined to define the current injections corresponding to the system nodes, in accordance with the components connected to each node. Thus the net current injections for all nodes of a nb-bus system can be expressed as a set of nonlinear equations that can be solved using the Newton–Raphson method. These equations are called the current injection mismatches during the iterative solution process. Rectangular coordinates are used to represent all phasor quantities. Thus the real and imaginary terms of the current injection mismatches can be written as

$$\Delta I_{\mathrm{Re}_k}^d = \frac{P_k^d\left(V_{\mathrm{Re}_k}^d - V_{\mathrm{Re}_k}^n\right) + Q_k^d\left(V_{\mathrm{Im}_k}^d - V_{\mathrm{Im}_k}^n\right)}{\left(V_{\mathrm{Re}_k}^d - V_{\mathrm{Re}_k}^n\right)^2 + \left(V_{\mathrm{Im}_k}^d - V_{\mathrm{Im}_k}^n\right)^2} - \sum_{t\in\alpha_p}\left(G_{kk}^{dt}V_{\mathrm{Re}_k}^t - B_{kk}^{dt}V_{\mathrm{Im}_k}^t\right) - \sum_{\substack{i\in\Omega_k\\ i\neq k}}\sum_{t\in\alpha_p}\left(G_{ki}^{dt}V_{\mathrm{Re}_i}^t - B_{ki}^{dt}V_{\mathrm{Im}_i}^t\right) \quad (16)$$

$$\Delta I_{\mathrm{Im}_k}^d = \frac{P_k^d\left(V_{\mathrm{Im}_k}^d - V_{\mathrm{Im}_k}^n\right) - Q_k^d\left(V_{\mathrm{Re}_k}^d - V_{\mathrm{Re}_k}^n\right)}{\left(V_{\mathrm{Re}_k}^d - V_{\mathrm{Re}_k}^n\right)^2 + \left(V_{\mathrm{Im}_k}^d - V_{\mathrm{Im}_k}^n\right)^2} - \sum_{t\in\alpha_p}\left(B_{kk}^{dt}V_{\mathrm{Re}_k}^t + G_{kk}^{dt}V_{\mathrm{Im}_k}^t\right) + \sum_{\substack{i\in\Omega_k\\ i\neq k}}\sum_{t\in\alpha_p}\left(B_{ki}^{dt}V_{\mathrm{Re}_i}^t + G_{ki}^{dt}V_{\mathrm{Im}_i}^t\right) \quad (17)$$

$$\Delta I_{\mathrm{Re}_k}^n = -\left(I_{\mathrm{Re}_k,\mathrm{lg}}^a + I_{\mathrm{Re}_k,\mathrm{lg}}^b + I_{\mathrm{Re}_k,\mathrm{lg}}^c\right) - \sum_{t\in\alpha_p}\left(G_{kk}^{nt}V_{\mathrm{Re}_k}^t - B_{kk}^{nt}V_{\mathrm{Im}_k}^t\right) - \sum_{\substack{i\in\Omega_k\\ i\neq k}}\sum_{t\in\alpha_p}\left(G_{ki}^{nt}V_{\mathrm{Re}_i}^t - B_{ki}^{nt}V_{\mathrm{Im}_i}^t\right) \quad (18)$$

$$\Delta I_{\mathrm{Im}_k}^n = -\left(I_{\mathrm{Im}_k,\mathrm{lg}}^a + I_{\mathrm{Im}_k,\mathrm{lg}}^b + I_{\mathrm{Im}_k,\mathrm{lg}}^c\right) - \sum_{t\in\alpha_p}\left(B_{kk}^{nt}V_{\mathrm{Re}_k}^t + G_{kk}^{nt}V_{\mathrm{Im}_k}^t\right) - \sum_{\substack{i\in\Omega_k\\ i\neq k}}\sum_{t\in\alpha_p}\left(B_{ki}^{nt}V_{\mathrm{Re}_i}^t + G_{ki}^{nt}V_{\mathrm{Im}_i}^t\right). \quad (19)$$

To apply Newton's method, (16)–(19) are linearized, leading to the following matrix system, that is solved in the iterative process:

$$\begin{bmatrix} \Delta I_{\mathrm{Im}_1}^{abcn} \\ \Delta I_{\mathrm{Re}_1}^{abcn} \\ \hline \Delta I_{\mathrm{Im}_2}^{abcn} \\ \Delta I_{\mathrm{Re}_2}^{abcn} \\ \hline \vdots \\ \hline \Delta I_{\mathrm{Im}_{nb}}^{abcn} \\ \Delta I_{\mathrm{Re}_{nb}}^{abcn} \end{bmatrix} = \left[\begin{array}{c|c|c|c} (J_{11})^{abcn} & (J_{12})^{abcn} & \cdots & (J_{1nb})^{abcn} \\ \hline (J_{21})^{abcn} & (J_{22})^{abcn} & \cdots & (J_{2nb})^{abcn} \\ \hline \vdots & \vdots & \vdots & \vdots \\ \hline (J_{nb1})^{abcn} & (J_{nb2})^{abcn} & \cdots & (J_{nbnb})^{abcn} \end{array}\right] \times \begin{bmatrix} \Delta V_{\mathrm{Re}_1}^{abcn} \\ \Delta V_{\mathrm{Im}_1}^{abcn} \\ \hline \Delta V_{\mathrm{Re}_2}^{abcn} \\ \Delta V_{\mathrm{Im}_2}^{abcn} \\ \hline \vdots \\ \hline \Delta V_{\mathrm{Re}_{nb}}^{abcn} \\ \Delta V_{\mathrm{Im}_{nb}}^{abcn} \end{bmatrix}. \quad (20)$$

It is seen that each current injection mismatch is expressed as a vector in which the imaginary part is the first component and the real part is the second. As for the voltage, the order is opposite. This procedure has been adopted to retain diagonal dominance of the Jacobian matrix [7].

The off-diagonal elements in (20) are 8×8 blocks and have the following composition:

$$(J_{ki})^{abcn} = \begin{bmatrix} B_{ki}^{aa} & B_{ki}^{ab} & B_{ki}^{ac} & B_{ki}^{an} & G_{ki}^{aa} & G_{ki}^{ab} & G_{ki}^{ac} & G_{ki}^{an} \\ B_{ki}^{ba} & B_{ki}^{bb} & B_{ki}^{bc} & B_{ki}^{bn} & G_{ki}^{ba} & G_{ki}^{bb} & G_{ki}^{bc} & G_{ki}^{bn} \\ B_{ki}^{ca} & B_{ki}^{cb} & B_{ki}^{cc} & B_{ki}^{cn} & G_{ki}^{ca} & G_{ki}^{cb} & G_{ki}^{cc} & G_{ki}^{cn} \\ B_{ki}^{na} & B_{ki}^{nb} & B_{ki}^{nc} & B_{ki}^{nn} & G_{ki}^{na} & G_{ki}^{nb} & G_{ki}^{nc} & G_{ki}^{nn} \\ G_{ki}^{aa} & G_{ki}^{ab} & G_{ki}^{ac} & G_{ki}^{an} & -B_{ki}^{aa} & -B_{ki}^{ab} & -B_{ki}^{ac} & -B_{ki}^{an} \\ G_{ki}^{ba} & G_{ki}^{bb} & G_{ki}^{bc} & G_{ki}^{bn} & -B_{ki}^{ba} & -B_{ki}^{bb} & -B_{ki}^{bc} & -B_{ki}^{bn} \\ G_{ki}^{ca} & G_{ki}^{cb} & G_{ki}^{cc} & G_{ki}^{cn} & -B_{ki}^{ca} & -B_{ki}^{cb} & -B_{ki}^{cc} & -B_{ki}^{cn} \\ G_{ki}^{na} & G_{ki}^{nb} & G_{ki}^{nc} & G_{ki}^{nn} & -B_{ki}^{na} & -B_{ki}^{nb} & -B_{ki}^{nc} & -B_{ki}^{nn} \end{bmatrix}. \quad (21)$$

Also for the diagonal elements, two terms, formed by 8×8 blocks, can be identified as (22) at the bottom of the next page.

It is clear that the off-diagonal elements of the Jacobian matrix in (21), and the first term of the diagonal elements in (22), are identical to the corresponding elements of the nodal admittance matrix and thus will remain constant throughout the iterative solution process. The second matrix in (22) reflects contributions from generators and or loads and will depend on the model and type of connection. As an example, for a ZIP, wye-connected load model, the second term of the diagonal element in (22), using (14) and (15), is derived in (23)–(26) at the bottom of the next page.

The system of equations to be solved for an nb bus system will have order $8 \cdot nb$, and the Jacobian matrix will retain the sparse structure of the nodal admittance matrix.

B. Representation of Controls

The procedure to incorporate control devices and other forms of controls in TCIM has been described in [8] and [9]. The same idea is applied in FCIM: control devices are modeled using additional equations to represent the control actions, resulting in an enlarged Jacobian matrix. The full Newton method is then applied to find the solution. An overview of two of the controls developed for FCIM is presented here: an improvement in the PV bus representation and an induction machine control.

1) PV Bus—Improvement: The basic representation of PV buses has been described in [16], where it was assumed that voltage-controlled buses were solid-grounded, wye-connected. In order to allow for neutrals that are either ungrounded or connected to ground through an impedance as shown in Fig. 1, the PV buses representation was extended and is presented next.

$$(J_{kk})^{abcn} = \begin{bmatrix} B_{kk}^{aa} & B_{kk}^{ab} & B_{kk}^{ac} & B_{kk}^{an} & G_{kk}^{aa} & G_{kk}^{ab} & G_{kk}^{ac} & G_{kk}^{an} \\ B_{kk}^{ba} & B_{kk}^{bb} & B_{kk}^{bc} & B_{kk}^{bn} & G_{kk}^{ba} & G_{kk}^{bb} & G_{kk}^{bc} & G_{kk}^{bn} \\ B_{kk}^{ca} & B_{kk}^{cb} & B_{kk}^{cc} & B_{kk}^{cn} & G_{kk}^{ca} & G_{kk}^{cb} & G_{kk}^{cc} & G_{kk}^{cn} \\ B_{kk}^{na} & B_{kk}^{nb} & B_{kk}^{nc} & B_{kk}^{nn} & G_{kk}^{na} & G_{kk}^{nb} & G_{kk}^{nc} & G_{kk}^{nn} \\ G_{kk}^{aa} & G_{kk}^{ab} & G_{kk}^{ac} & G_{kk}^{an} & -B_{kk}^{aa} & -B_{kk}^{ab} & -B_{kk}^{ac} & -B_{kk}^{an} \\ G_{kk}^{ba} & G_{kk}^{bb} & G_{kk}^{bc} & G_{kk}^{bn} & -B_{kk}^{ba} & -B_{kk}^{bb} & -B_{kk}^{bc} & -B_{kk}^{bn} \\ G_{kk}^{ca} & G_{kk}^{cb} & G_{kk}^{cc} & G_{kk}^{cn} & -B_{kk}^{ca} & -B_{kk}^{cb} & -B_{kk}^{cc} & -B_{kk}^{cn} \\ G_{kk}^{na} & G_{kk}^{nb} & G_{kk}^{nc} & G_{kk}^{nn} & -B_{kk}^{na} & -B_{kk}^{nb} & -B_{kk}^{nc} & -B_{kk}^{nn} \end{bmatrix} + \begin{bmatrix} -e_k^a & & & e_k^a & -f_k^a & & & f_k^a \\ & -e_k^b & & e_k^b & & -f_k^b & & f_k^b \\ & & -e_k^c & e_k^c & & & -f_k^c & f_k^c \\ e_k^a & e_k^b & e_k^c & -e_k^a - e_k^b - e_k^c & f_k^a & f_k^b & f_k^c & -f_k^a - f_k^b - f_k^c \\ -g_k^a & & & g_k^a & -h_k^a & & & h_k^a \\ & -g_k^b & & g_k^b & & -h_k^b & & h_k^b \\ & & -g_k^c & g_k^c & & & -h_k^c & h_k^c \\ g_k^a & g_k^b & g_k^c & -g_k^a - g_k^b - g_k^c & h_k^a & h_k^b & h_k^c & -h_k^a - h_k^b - h_k^c \end{bmatrix} \tag{22}$$

$$e = \frac{\left(Q_k'^d\right)\left(V_{\mathrm{Re}_k}^d - V_{\mathrm{Re}_k}^n\right)^2 - \left(Q_k'^d\right)\left(V_{\mathrm{Im}_k}^d - V_{\mathrm{Im}_k}^n\right)^2 - 2\left(P_k'^d\right)\left(V_{\mathrm{Re}_k}^d - V_{\mathrm{Re}_k}^n\right)\left(V_{\mathrm{Im}_k}^d - V_{\mathrm{Im}_k}^n\right)}{\left[\left(V_{\mathrm{Re}_k}^d - V_{\mathrm{Re}_k}^n\right)^2 + \left(V_{\mathrm{Im}_k}^d - V_{\mathrm{Im}_k}^n\right)^2\right]^2} + \frac{\left(P_{I_k}^d\right)\left(V_{\mathrm{Re}_k}^d - V_{\mathrm{Re}_k}^n\right)\left(V_{\mathrm{Im}_k}^d - V_{\mathrm{Im}_k}^n\right) + \left(Q_{I_k}^d\right)\left(V_{\mathrm{Im}_k}^d - V_{\mathrm{Im}_k}^n\right)^2}{\left[\left(V_{\mathrm{Re}_k}^d - V_{\mathrm{Re}_k}^n\right)^2 + \left(V_{\mathrm{Im}_k}^d - V_{\mathrm{Im}_k}^n\right)^2\right]^{\frac{3}{2}}} + Q_{Z_k}^d \tag{23}$$

$$f = \frac{\left(P_k'^d\right)\left(V_{\mathrm{Re}_k}^d - V_{\mathrm{Re}_k}^n\right)^2 - \left(P_k'^d\right)\left(V_{\mathrm{Im}_k}^d - V_{\mathrm{Im}_k}^n\right)^2 + 2\left(Q_k'^d\right)\left(V_{\mathrm{Re}_k}^d - V_{\mathrm{Re}_k}^n\right)\left(V_{\mathrm{Im}_k}^d - V_{\mathrm{Im}_k}^n\right)}{\left[\left(V_{\mathrm{Re}_k}^d - V_{\mathrm{Re}_k}^n\right)^2 + \left(V_{\mathrm{Im}_k}^d - V_{\mathrm{Im}_k}^n\right)^2\right]^2} + - \frac{\left(Q_{I_k}^d\right)\left(V_{\mathrm{Re}_k}^d - V_{\mathrm{Re}_k}^n\right)\left(V_{\mathrm{Im}_k}^d - V_{\mathrm{Im}_k}^n\right) + \left(P_{I_k}^d\right)\left(V_{\mathrm{Re}_k}^d - V_{\mathrm{Re}_k}^n\right)^2}{\left[\left(V_{\mathrm{Re}_k}^d - V_{\mathrm{Re}_k}^n\right)^2 + \left(V_{\mathrm{Im}_k}^d - V_{\mathrm{Im}_k}^n\right)^2\right]^{\frac{3}{2}}} - P_{Z_k}^d \tag{24}$$

$$g = \frac{-\left(P_k'^d\right)\left(V_{\mathrm{Re}_k}^d - V_{\mathrm{Re}_k}^n\right)^2 + \left(P_k'^d\right)\left(V_{\mathrm{Im}_k}^d - V_{\mathrm{Im}_k}^n\right)^2 - 2\left(Q_k'^d\right)\left(V_{\mathrm{Re}_k}^d - V_{\mathrm{Re}_k}^n\right)\left(V_{\mathrm{Im}_k}^d - V_{\mathrm{Im}_k}^n\right)}{\left[\left(V_{\mathrm{Re}_k}^d - V_{\mathrm{Re}_k}^n\right)^2 + \left(V_{\mathrm{Im}_k}^d - V_{\mathrm{Im}_k}^n\right)^2\right]^2} + \frac{\left(Q_{I_k}^d\right)\left(V_{\mathrm{Re}_k}^d - V_{\mathrm{Re}_k}^n\right)\left(V_{\mathrm{Im}_k}^d - V_{\mathrm{Im}_k}^n\right) - \left(P_{I_k}^d\right)\left(V_{\mathrm{Im}_k}^d - V_{\mathrm{Im}_k}^n\right)^2}{\left[\left(V_{\mathrm{Re}_k}^d - V_{\mathrm{Re}_k}^n\right)^2 + \left(V_{\mathrm{Im}_k}^d - V_{\mathrm{Im}_k}^n\right)^2\right]^{\frac{3}{2}}} - P_{Z_k}^d \tag{25}$$

$$h = \frac{\left(Q_k'^d\right)\left(V_{\mathrm{Re}_k}^d - V_{\mathrm{Re}_k}^n\right)^2 - \left(Q_k'^d\right)\left(V_{\mathrm{Im}_k}^d - V_{\mathrm{Im}_k}^n\right)^2 - 2\left(P_k'^d\right)\left(V_{\mathrm{Re}_k}^d - V_{\mathrm{Re}_k}^n\right)\left(V_{\mathrm{Im}_k}^d - V_{\mathrm{Im}_k}^n\right)}{\left[\left(V_{\mathrm{Re}_k}^d - V_{\mathrm{Re}_k}^n\right)^2 + \left(V_{\mathrm{Im}_k}^d - V_{\mathrm{Im}_k}^n\right)^2\right]^2} + \frac{\left(P_{I_k}^d\right)\left(V_{\mathrm{Re}_k}^d - V_{\mathrm{Re}_k}^n\right)\left(V_{\mathrm{Im}_k}^d - V_{\mathrm{Im}_k}^n\right) - \left(Q_{I_k}^d\right)\left(V_{\mathrm{Re}_k}^d - V_{\mathrm{Re}_k}^n\right)^2}{\left[\left(V_{\mathrm{Re}_k}^d - V_{\mathrm{Re}_k}^n\right)^2 + \left(V_{\mathrm{Im}_k}^d - V_{\mathrm{Im}_k}^n\right)^2\right]^{\frac{3}{2}}} - Q_{Z_k}^d \tag{26}$$

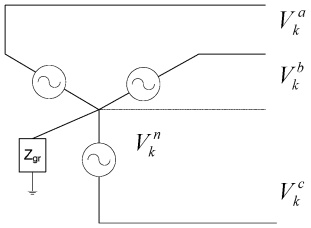

Fig. 1. PV bus with neutral grounding.

To implement this control the reactive power generations per phase are represented as new state variables $Q^a_{G_k}$, $Q^b_{G_k}$ and $Q^c_{G_k}$ for each PV bus k. Three new equations to define the phase to neutral voltage control, considering the neutral voltage, are needed, as follows:

$$V^2_{esp,k} - \left(V^a_{\mathrm{Re}_k} - V^n_{\mathrm{Re}_k}\right)^2 - \left(V^a_{\mathrm{Im}_k} - V^n_{\mathrm{Im}_k}\right)^2 = 0 \quad (27)$$

$$V^2_{esp,k} - \left(V^b_{\mathrm{Re}_k} - V^n_{\mathrm{Re}_k}\right)^2 - \left(V^b_{\mathrm{Im}_k} - V^n_{\mathrm{Im}_k}\right)^2 = 0 \quad (28)$$

$$V^2_{esp,k} - \left(V^c_{\mathrm{Re}_k} - V^n_{\mathrm{Re}_k}\right)^2 - \left(V^c_{\mathrm{Im}_k} - V^n_{\mathrm{Im}_k}\right)^2 = 0 \quad (29)$$

where $V_{esp,k}$ is the specified phase-to-neutral voltage magnitude at bus k.

Remote voltage control can be included in a similar way.

2) Induction Machines: Induction machines can be incorporated in the power flow equations using the nodal admittance matrix that can be obtained from the equivalent circuit [24]. The equivalent circuits for positive and negative sequences can be reduced to admittances $y_1(s)$ and $y_2(s)$ respectively, and these depend on the slip. The zero sequence admittance is made equal to zero, as there are normally no neutral connections to induction machines. The sequence admittance matrix $\mathbf{Y}^{012}(\mathrm{s})$ of the machine model will be diagonal. Since the proposed method uses phase coordinates, the three-phase admittance matrix $\mathbf{Y}^{\mathrm{abc}}(\mathrm{s})$ can be obtained by applying the synthesis symmetric component transformation to $\mathbf{Y}^{012}(\mathbf{s})$. It is known that the positive and negative sequence equivalent circuits will result in different values for the admittances $y_1(s)$ and $y_2(s)$. Thus the induction machine admittance matrix $\mathbf{Y}^{\mathrm{abc}}(\mathrm{s})$ will be full and asymmetric, and all elements will depend on the slip s.

When the machine is not operated at constant slip, it is necessary to define the kind of operation to be adopted. Three possibilities have been considered: i. constant electrical power input/output, ii. constant mechanical power output/input and iii. constant mechanical torque output/input. Thus the extra equations needed to represent the machine control can be written in terms of the slip s as a new state variable. For example, for constant electrical power input the new equation is written as follows:

$$P^{ele-in}_{esp} - P^{ele-in}_{calc} = 0$$

$$P^{ele-in}_{esp} - \mathrm{Re}\left(\left[V^{abc}_m\right]^t \cdot \left(\left[Y^{abc}(s)\right] \cdot \left[V^{abc}_m\right]\right)^*\right) = 0 \quad (30)$$

where P^{ele-in}_{esp} is the specified active electrical power input to the induction machine at bus m, and P^{ele-in}_{calc} is the active power calculated in terms of the slip s and the other state variables. Once convergence is achieved, the value of the slip is obtained and the input reactive power can be calculated.

If the machine is run at constant slip, the admittance matrix $\mathrm{Y}^{\mathrm{abc}}(\mathrm{s})$ will remain constant, and can be incorporated directly into the Jacobian. Thus new state variables and extra equations are not needed in this case.

C. FCIM Proposed Algorithm

Step 1) Initialize all state variables (e.g., complex voltages, slip, etc.) and iteration count $(\mathrm{h} = 0)$.

Step 2) Calculate the current injection mismatches $\Delta I^{(h)} = [\Delta I^s_{\mathrm{Im}}\ \Delta I^s_{\mathrm{Re}}]^t$ for all system nodes (16)–(19) and control equations $(\Delta\mathrm{control}^{(\mathrm{h})})$, for example (27)–(29), (30).

Step 3) Test for convergence. If max $\{|\Delta \mathrm{I}^{(h)}|\} \leq \epsilon$ and max $\{|\Delta\mathrm{control}^{(\mathrm{h})}|\} \leq \epsilon$, go to step 7; else, go to step 4.

Step 4) Assemble the Jacobian $(\mathrm{J}^{(\mathrm{h})})$ matrix (enlarged if there are control equations).

Step 5) Solve the system of equations.

Step 6) Update all the state variables. For example, slip: $(s)^{(h+1)} = (s)^{(h)} + (\Delta s)^{(h)}$; and complex voltages of the following system:

$$\left(V^s_{\mathrm{Re}_k}\right)^{(h+1)} = \left(V^s_{\mathrm{Re}_k}\right)^{(h)} + \left(\Delta V^s_{\mathrm{Re}_k}\right)^{(h)}$$

$$\left(V^s_{\mathrm{Im}_k}\right)^{(h+1)} = \left(V^s_{\mathrm{Im}_k}\right)^{(h)} + \left(\Delta V^s_{\mathrm{Im}_k}\right)^{(h)}.$$

Increment the iteration count $h = h + 1$;
Return to step 2.

Step 7) Exit from the iterative process and print the results.

III. Applications

The program developed based on the proposed methodology has been tested using practical feeders operated by a distribution utility in Brazil, as well as the IEEE test feeders [18]–[23], that have been developed for the purpose of validation of distribution systems analysis software [19]. Recently some of these systems have been extended to include a center tapped wye-delta transformer bank, and induction machines [20]–[23]. A summary of results achieved using FCIM for some of these systems are presented in this section.

In some cases the available data was converted or adapted to phase coordinates as the FCIM simulation tool requires the data in this format.

The current tolerance for convergence was set at 10^{-4} p.u.

A. IEEE 34-Node Test Feeder With Induction Generators

The one line diagram of this system as proposed in [23] is shown in Fig. 2, and is based on the IEEE 34-Node Test Feeder [18]. Two three-phase induction generators with step-down transformers have been added, for the purpose of testing induction generator models. The system is unbalanced and each generator is to supply constant 660 kW to the feeder.

Since the electrical power output from each generator is considered constant, the procedure i described in Section II-B2 was applied.

The distributed specified loads were equally divided between the "from" bus and the "to" bus of the respective line section.

Three different connections (A_1—Grounded wye-wye, A_2—Grounded wye-ungrounded wye and A_3—Grounded wye-delta) of the two induction generators transformers were

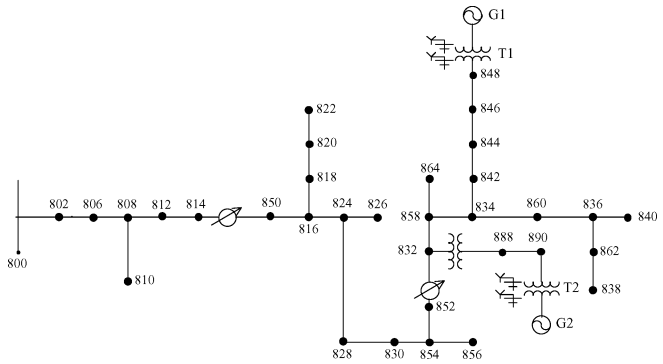

Fig. 2. The 34-node test feeder with induction generators.

TABLE I
LINE CURRENTS

Line	Ia (A)	θa (°)	Ib (A)	θb (°)	Ic (A)	θc (°)
800-802	36.895	-57.301	29.048	177.145	21.859	57.672
814r-850	35.353	-57.300	25.835	172.895	20.237	54.739
846-848	13.147	176.796	12.736	59.146	13.582	-65.335
888-890	92.595	-97.946	94.678	139.397	89.869	19.561
T1-G1	854.780	-146.969	893.795	92.453	867.305	-29.497
T2-G2	941.934	-137.637	975.915	101.169	942.025	-20.035

TABLE II
PHASE TO GROUND NODAL VOLTAGES

Bus	Va (kV)	θa (°)	Vb (kV)	θb (°)	Vc (kV)	θc (°)
800	15.095	0.000	15.095	-120.000	15.095	120.000
814	14.020	1.616	14.572	-119.219	14.654	121.554
814r	14.632	1.616	14.710	-119.219	14.695	121.554
852	14.261	3.748	14.292	-117.746	14.842	122.821
852r	14.817	3.748	14.843	-117.746	14.842	122.821
832	14.817	3.748	14.843	-117.746	14.842	122.822
836	14.775	3.835	14.792	-117.743	14.806	122.787
848	14.804	3.858	14.815	-117.712	14.834	122.813
888	2.361	5.838	2.364	-115.555	2.370	124.915
890	2.284	12.102	2.273	-109.815	2.289	130.979
G1	0.282	6.214	0.282	-114.826	0.281	125.505
G2	0.260	14.860	0.259	-106.375	0.259	134.163

Bus	Vgn (kV)	θgn (°)
T1	0.00122	-65.005
T2	0.00152	-61.469

simulated. The results obtained with FCIM for the connection A_1 are in very close agreement with the calculations reported in [23].

Tables I and II show the results obtained with FCIM for the connection A_2, including the neutral voltages of the two ungrounded wye transformers.

Induction generator 1 results: $\text{slip} = -0.7523158\%$
Stator Complex Power Input: -660.000 +j 327.236 kVA
Converted Shaft Power: -669.222 kW

Induction generator 2 results: $\text{slip} = -0.9123154\%$
Stator Complex Power Input: -660.000 +j 335.673 kVA
Converted Shaft Power: -671.117 kW

In this case the power flow converged in four iterations of the full Newton method.

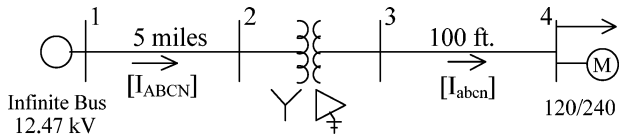

Fig. 3. Center tapped wye-delta transformer test case.

TABLE III
PHASE TO GROUND VOLTAGES

Bus	V_{AG} (kV)	θ_A (°)	V_{BG} (kV)	θ_B (°)	V_{CG} (kV)	θ_C (°)
1	7.200	0.00	7.200	-120.00	7.200	120.00
2	7.194	-0.05	7.194	-120.01	7.197	119.97
3	0.117	-0.51	0.117	179.52	0.204	89.86
4	0.116	-0.25	0.115	179.42	0.203	89.85

TABLE IV
MAGNITUDE OF LINE CURRENTS

Line	I_A (A)	I_B (A)	I_C (A)	I_N (A)
1-2	2.745	1.760	1.609	0.040
3-4	114.555	138.025	58.868	10.792

TABLE V
MOTOR INPUT CURRENTS

IM_A (A)	θ_A (°)	IM_B (A)	θ_B (°)	IM_C (A)	θ_C (°)
54.642	-66.480	55.537	178.137	58.893	55.092

B. IEEE Center Tapped Wye-Delta Transformer Test Case

The system shown in Fig. 3 is based on the IEEE Four-Node Test Feeder [18], that was created for testing four wire delta transformer models, where a more complete model was included: the wye-delta transformer bank with a center-tap in one leg of the delta secondary [20]. According to [21] this presents a challenge to designers of distribution system analysis software. The center tap is grounded, which shifts the secondary side voltage reference to an unusual location for three-phase circuit analysis. One phase is significantly higher in voltage with respect to ground resulting in a "crazy" leg.

In this test case the induction motor slip was considered fixed at 3.5%, therefore the constant admittance model has been used for the motor as explained in Section II-B2.

The following transformer connections were tested: B_1—Ungrounded wye-delta; B_2—Grounded wye-delta; B_3—Leading open wye-open delta; B4—Lagging open wye-open delta. Some selected results obtained with FCIM, for case B1, are given in Tables III–V.

The wye transformer neutral voltage V_{NG} is $63.26\angle 3.047°\text{V}$ which reflects the neutral shift due to the unbalanced operation, the secondary center tap ground current is $9.86\angle 129.28°\text{A}$.

Induction motor results for $\text{slip} = 3.5\% = 0.035$:
Stator Input Complex Power: 18.827 + j 12.794 kVA
Converted Shaft Power: 17.454 kW

All the results obtained for this system are in close agreement with those reported in [20].

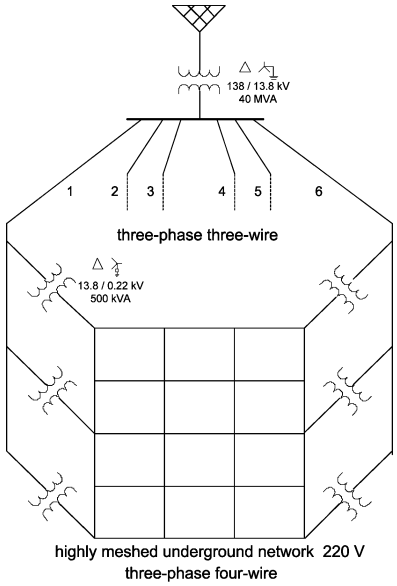

Fig. 4. Brazilian distribution system.

TABLE VI
LINE CURRENTS

Line	Ia (A)	Ib (A)	Ic (A)
Substation@138 kV	78.745	93.558	87.966
Feeder 1@13,8 kV	134.616	145.754	123.460
Feeder 2@13,8 kV	118.660	129.505	110.447
Feeder 3@13,8 kV	133.247	146.070	123.400
Feeder 4@13,8 kV	119.217	130.170	113.329
Feeder 5@13,8 kV	148.391	162.123	137.245
Feeder 6@13,8 kV	133.421	146.004	124.118

C. Practical Feeder—Brazilian Distribution System

To verify the efficiency and performance of the proposed methodology in large scale meshed systems, the algorithm was applied to a Brazilian utility distribution system (138/13.8/0.22 kV). The network consists of the utility substation (138 kV), one OLTC 40MVA 138/13.8 kV step-down transformer, six 13.8 kV three-phase three-wire overhead feeders, 56 500 kVA 13.8/0.22 kV step-down transformers, and a 220 V three-phase four-wire highly meshed underground network. This system has 482 buses, total active load of 14.83 MW, and total reactive load of 11.12 Mvar. A very simplified representation of this system is shown in Fig. 4.

A total of 702 series elements were applied to model this system including lines, transformers and switches. The neutral conductors are grounded by 0.5–3 ohms resistors in some points of the low voltage network. The system is unbalanced.

Using FCIM convergence was achieved in only five iterations when the OLTC transformer was set to control the voltage at 13.8 kV. The simulation timings on a Pentium IV, 3.2 MHz and 512 MB, was 0.52 s for this first case, and selected results are presented in Table VI and Fig. 5–8.

The values marked by "o" in Fig. 5 are the 13.8 kV bus calculated voltages and the values marked by "x" are the 220 V bus calculated voltages. It is seen that the highly meshed network does not show any considerable voltage drops in the 13.8 kV feeders, which would normally be present in radial topologies. As was to be expected, the low voltage network shows higher voltage drops when compared to the 13.8 kV feeders. The neutral voltages are shown in Fig. 6.

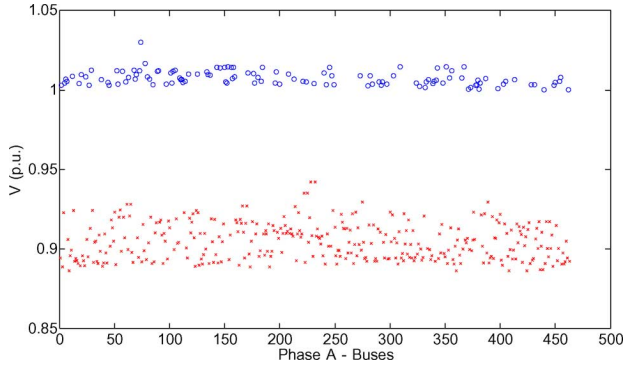

Fig. 5. Phase-A voltages.

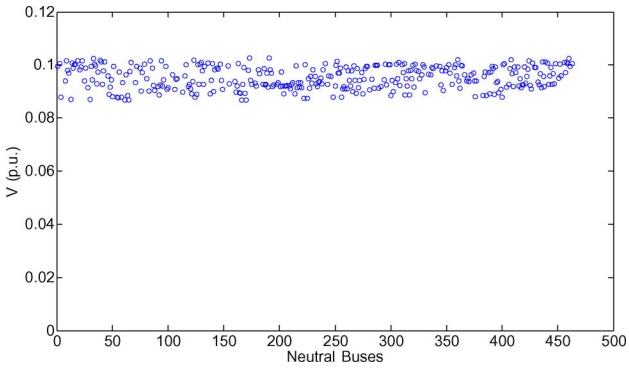

Fig. 6. Neutral voltages.

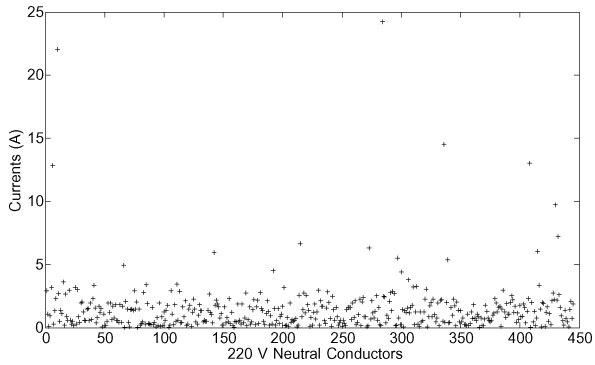

Fig. 7. The 220 V neutral conductors currents.

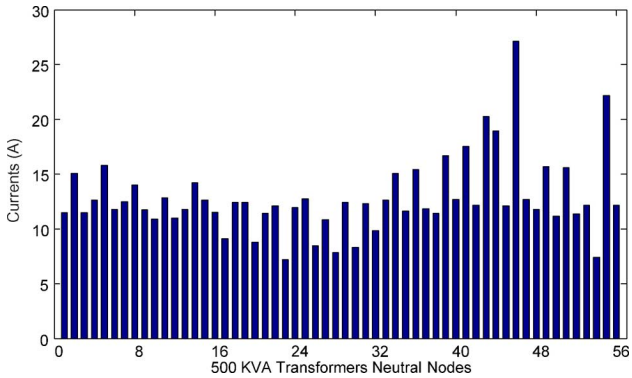

Fig. 8. Transformers neutral grounding currents.

TABLE VII
INDUCTION GENERATORS RESULTS

	Machine 1		Machine 2		Machine 3		Machine 4	
Ia (A / °)	1270	-124	1336	-124	1402	-124	1470	-124
Ib (A / °)	1277	116	1344	116	1409	116	1479	116
Ic (A / °)	1277	-4	1342	-4	1407	-4	1477	-4
s (%)	-0.5987946		-0.6341572		-0.6687410		-0.7071461	
Active Power (kW)	950.00		1000.00		1050.00		1100.00	
Reactive Power (kvar)	479.32		499.85		521.82		545.02	
Stator I+ (A)	1275.04		1340.96		1406.46		1475.78	
Stator I- (A)	4.94		4.68		4.44		4.89	
Rotor I+ (A)	1190.89		1257.55		1323.45		1393.15	
Rotor I- (A)	4.80		4.55		4.31		4.75	
Axis Torque (kWN)	2.53		2.66		2.80		2.94	

TABLE VIII
LINE CURRENTS WITH INDUCTION GENERATORS

Line	Ia (A)	Ib (A)	Ic (A)
Substation@138 kV	73.190	75.114	73.500
Feeder 1@13,8 kV	109.150	108.870	105.672
Feeder 2@13,8 kV	119.344	119.129	117.343
Feeder 3@13,8 kV	107.425	108.830	105.171
Feeder 4@13,8 kV	93.410	94.210	91.557
Feeder 5@13,8 kV	148.937	148.924	146.390
Feeder 6@13,8 kV	107.362	108.167	105.326

TABLE IX
CASES COMPILATION

Case	Substation (MW)	Substation (Mvar)	Losses (kW)
Base	15.127	14.110	285.9
With Induction Generators	10.943	13.874	208.9

The 220 V underground network neutral currents are shown in Fig. 7 whereas Fig. 8 shows the currents flowing in the neutral grounding impedances of the 500 kVA transformers.

In another test, to simulate DG, four two-pole 1200 kVA 460 V induction machines have been added to the system at buses 129, 104, 109 and 125. The machines were connected by means of four 1200 kVA, 13.8/0.48 kV step-down transformers. These buses are situated in feeders 1, 3, 4 and 6, respectively. It was assumed that the machines were operating as induction generators at constant electrical power output; the values taken for the tests were: 950, 1000, 1050 e 1100 kW. Each machine had a 450 kvar grounded-wye capacitor bank connected to its terminals.

Some selected results for this case are presented in Tables VII and VIII and in Figs. 9–12.

Comparing the results in Figs. 5–8 with the corresponding values in Figs. 9–12, it will be seen that the combined action of the distributed induction generators and capacitor banks have improved the voltage levels in the 220 V underground network, and have also decreased the neutral currents as well as the neutral shifts. The cases compilation are shown in Table IX.

D. Comparison With FBS

The computational efficiency of the proposed methodology has been compared with the well-known forward-backward sweep (FBS) method [3]. This method was extended to include

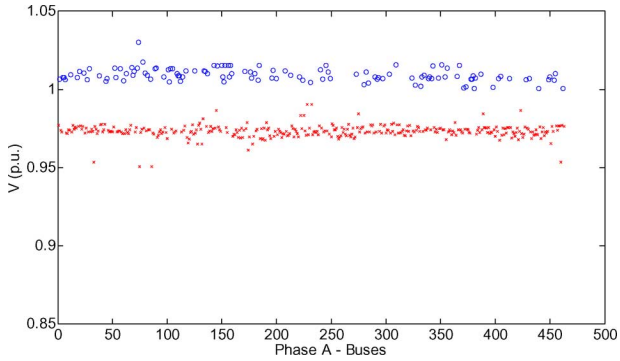

Fig. 9. Phase-A voltages with DG.

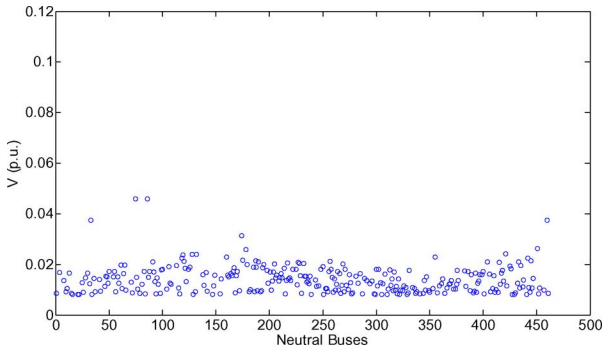

Fig. 10. Neutral voltages with DG.

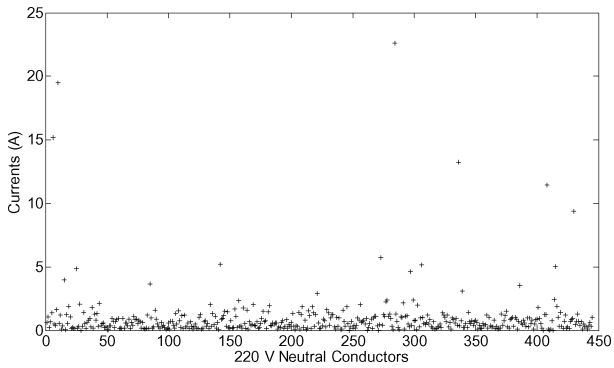

Fig. 11. Neutral conductors currents with DG.

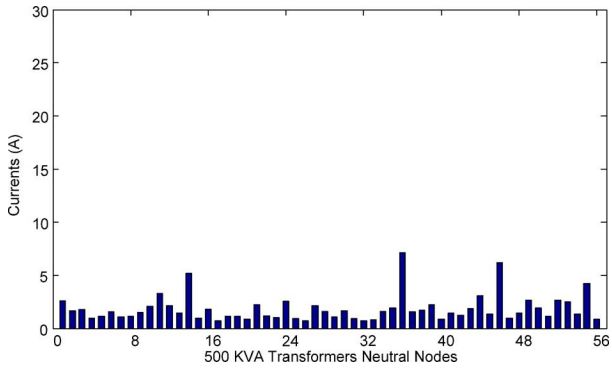

Fig. 12. Transformers neutral grounding currents with DG.

representation of the neutral conductor. As described in [16] FBS requires a preliminary procedure to identify the systems

TABLE X
RESULTS FOR THE 10 103 BUSES SYSTEM, TIME IN SECONDS

FBS		FCIM	
Number of iterations	Total time	Number of iterations	Total time
41	4.034	4	2.326
Average iteration time			
0.098		0.582	
Layer identification time		Ordering time for FCIM	
9.71		0.351	

layers. Once this is determined, the algorithm performs backward and forward sweeps until convergence is achieved.

Neutral conductors were added to the 10 103-bus distribution system described in [16] and both FBS and FCIM routines were applied using a 3.2 MHz, 512 Mb RAM, Pentium computer and the main performance data are given in Table X. It is seen that the average iteration time of FBS is quite small. However, since both the number of iterations and the layer identification time required by FBS are very large for this system, the FBS total solution time is considerably larger than FCIM. Some other comparisons between the current injection method and FBS for three-phase systems are described in [16].

IV. CONCLUSIONS

This work proposed an extension of the TCIM of power flow analysis. This extended formulation, has been named FCIM. One the main advantages of this modeling lies on the explicit representation of neutrals and groundings as well as on the direct calculation of neutral voltages and currents.

The method has been validated by comparisons with well-known distribution test feeders results reported in the literature. Convergence was achieved with no more than five iterations in all cases, which indicates the robustness of the method. This methodology is especially useful to solve systems with a large number of controls, very meshed or large scale systems.

The authors believe that FCIM will be of special assistance for the analysis of unbalanced distribution systems with neutral conductors, isolated or with any kind of grounding, and can be applied to solve both balanced and unbalanced systems, radial or meshed, with controls and distributed generation.

REFERENCES

[1] T. Chen and W. Yang, "Analysis of multi-grounded four-wire distribution systems considering the neutral grounding," *IEEE Trans. Power Del.*, vol. 16, no. 4, pp. 710–717, Oct. 2001.

[2] J. J. Allemong, R. J. Bennon, and P. W. Selent, "Multiphase power flow solutions using EMTP and Newtons method," *IEEE Trans. Power Syst.*, vol. 8, no. 4, pp. 1455–1462, Nov. 1993.

[3] C. S. Cheng and D. Shirmohammadi, "A three-phase power flow method for real-time distribution system analysis," *IEEE Trans. Power Syst.*, vol. 10, no. 2, pp. 671–679, May 1995.

[4] T. H. Chen *et al.*, "Distribution system power flow analysis-A rigid approach," *IEEE Trans. Power Del.*, vol. 6, no. 3, pp. 1146–1152, Jul. 1991.

[5] D. Rajicic, R. Ackovski, and R. Taleski, "Voltage correction power flow," *IEEE Trans. Power Del.*, vol. 9, no. 2, pp. 1056–1062, Apr. 1994.

[6] R. M. Ciric, A. P. Feltrin, and L. F. Ochoa, "Power flow in four-wire distribution networks—General approach," *IEEE Trans. Power Syst.*, vol. 18, no. 4, pp. 1283–1290, Nov. 2003.

[7] P. A. N. Garcia, J. L. R. Pereira, S. Carneiro, Jr., V. M. da Costa, and N. Martins, "Three-phase power flow calculations using the currents injection methods," *IEEE Trans. Power Syst.*, vol. 15, no. 2, pp. 508–514, May 2000.

[8] P. A. N. Garcia, J. L. R. Pereira, and S. Carneiro, Jr., "Voltage control devices models for distribution power flow analysis," *IEEE Trans. Power Syst.*, vol. 16, no. 4, pp. 586–594, Nov. 2001.

[9] P. A. N. Garcia, J. L. R. Pereira, and S. Carneiro, Jr., "Improvements in the representation of PV buses on three-phase distribution power flow," *IEEE Trans. Power Del.*, vol. 19, no. 2, pp. 894–896, Apr. 2004.

[10] G. X. Luo and A. Semlyen, "Efficient load flow for large weakly meshed networks," *IEEE Trans. Power Syst.*, vol. 5, no. 4, pp. 1309–1316, Nov. 1990.

[11] Y. Zhu and K. Tomsovic, "Adaptive power flow method for distribution system with dispersed generation," *IEEE Trans. Power Del.*, vol. 17, no. 3, pp. 822–827, Jul. 2002.

[12] R. Stoicescu, K. Miu, C. O. Nwankpa, D. Niebur, and X. Yang, "Three-phase converter models for unbalanced radial power-flow studies," *IEEE Trans. Power Syst.*, vol. 17, no. 4, pp. 1016–1021, Nov. 2002.

[13] P. Xiao, D. C. Yu, and W. Wa, "A unified three-phase transformer model for distribution load flow calculations," *IEEE Trans. Power Syst.*, vol. 21, no. 1, pp. 153–159, Feb. 2006.

[14] Z. Wang, F. Chen, and J. Li, "Implementing transformer nodal admittance matrices into backward-forward sweep-based power flow analysis for unbalanced radial distribution systems," *IEEE Trans. Power Syst.*, vol. 19, no. 4, pp. 1831–1836, Nov. 2004.

[15] L. R. Araujo, "Applications of oriented object modelling techniques in sparse linear systems," (in Portuguese) M.Sc. thesis, Federal Univ. Juiz de Fora, Juiz de Fora, MG, Brazil, Dec. 2000.

[16] L. R. Araujo, D. R. R. Penido, S. Carneiro, Jr., J. L. R. Pereira, and P. A. N. Garcia, "A comparative study on the performance of tcim full newton versus forward-backward power flow methods for large distribution systems," in *Proc. 2006 IEEE Power System Conf. Exhib.*, Atlanta, GA, Oct. 2006.

[17] D. R. R. Penido, L. R. Araujo, J. L. R. Pereira, P. A. N. Garcia, and S. Carneiro, Jr., "Four wire Newton-Raphson power flow based on the current injection method," in *Proc. 2004 IEEE Power System Conf. Exhib.*, New York, Oct. 2004.

[18] [Online]. Available: http://ewh.ieee.org/soc/pes/dsacom/testfeeders.html.

[19] W. H. Kersting, "Transformer model test system," in *Proc. 2003 IEEE Power Eng. Soc. Transmission and Distribution Conf.*, Dallas, TX, Sep. 2003.

[20] W. H. Kersting, "Center tapped wye-delta transformer test case," in *Proc. 2004 IEEE Power Eng. Soc. General Meeting*, Denver, CO, Jun. 2004.

[21] R. C. Dugan, "Experiences with the center-tapped Wye-delta transformer test case," in *Proc. 2004 IEEE Power Eng. Soc. General Meeting*, Denver, CO, Jun. 2004.

[22] R. C. Dugan, "Induction machine modeling for distribution system analysis—Test case description," in *Proc. 2006 IEEE Power Eng. Soc. Transmission and Distribution Conf.*, Dallas, TX, May 2006.

[23] R. C. Dugan and W. H. Kersting, "Induction machine test case for the 34-bus test feeder—Description," in *Proc. 2006 IEEE Power Eng. Soc. General Meeting*, Montreal, QC, Canada, Jun. 2006.

[24] D. R. R. Penido, L. R. Araujo, S. Carneiro, Jr., and J. L. R. Pereira, "Unbalanced three-phase distribution system load-flow studies including induction machines, panel on induction machine modeling for distribution system analysis," in *Proc. 2006 IEEE Power Eng. Soc. General Meeting*, Montreal, QC, Canada, Jun. 2006.

[25] P. M. Anderson, *Analysis of Faulted Power Systems*, ser. Power Systems Engineering. New York: IEEE Press, 1995, ch. 4.

Debora Rosana Ribeiro Penido (S'1999) was born in Brazil in 1978. She received the Electrical Engineer and M.Sc. degrees from the Federal University of Juiz de Fora (UFJF), Juiz de Fora, Brazil, in 2002 and 2004, respectively. She is pursuing the Ph.D. degree in electrical engineering at the Graduate School of Engineering (COPPE)/Federal University of Rio de Janeiro (UFRJ), Rio de Janeiro, Brazil.

Since 2003, she has been with the Transmission Department of the Brazilian Electrical Company-ELETROBRAS, Electrical Studies Division. Her research interests include models and analytical tools for distribution systems analysis and planning of transmission systems.

Leandro Ramos de Araujo was born in Brazil in 1974. He received the Electrical Engineer and M.Sc. degrees from the Federal University of Juiz de Fora (UFJF), Juiz de Fora, Brazil, in 1997 and 2000, respectively, and the Ph.D. degree in electrical engineering from the Graduate School of Engineering (COPPE)/Federal University of Rio de Janeiro (UFRJ), Rio de Janeiro, Brazil, in 2005.

From 2003 to 2005, he was with the Electrical Energy Research Center (CEPEL) of Brazilian Electrical Company-ELETROBRAS. Since 2005, he has been with the Brazilian Petroleum Company—PETROBRAS. His research interests include the development of tools for optimization and operation of transmission, distribution, and industrial systems.

Sandoval Carneiro, Jr. (M'78–SM'91) was born in Brazil in 1945. He received the Electrical Engineer degree from the Faculty of Electrical Engineering (FEI), of the Catholic University of São Paulo, São Paulo, Brazil, in 1968, the M.Sc. degree from the Graduate School of Engineering (COPPE)/Federal University of Rio de Janeiro (UFRJ), Rio de Janeiro, Brazil, in 1971, and the Ph.D. degree in electrical engineering from University of Nottingham, Nottingham,, U.K., in 1976.

Since 1971, he has been a Lecturer at the Federal University of Rio de Janeiro and in 1993 was promoted to Full Professor. From 1978 to 1979, he was Deputy-Director and from 1982 to 1985 Director of COPPE/UFRJ. From 1987 to 1988 and in 1994, he was Visiting Professor with the Department of Electrical Engineering of the University of British Columbia, Vancouver, BC, Canada. From October 1991 to June 1992, he was General Director of CAPES—Ministry of Education Agency for Academic Improvement. His research interests include electromagnetic transients simulations and models and analytical tools for distribution systems analysis.

Dr. Carneiro is a registered Professional Engineer in the State of Rio de Janeiro, Brazil.

Jose Luiz Rezende Pereira (M'85–SM'05) received the B.Sc. degree in 1975 from Federal University of Juiz de Fora, Juiz de Fora, Brazil, the M.Sc. degree in 1978 from COPPE-Federal University of Rio de Janeiro, Rio de Janeiro, Brazil, and the Ph.D. degree in 1988 from the University of Manchester Institute of Science and Technology, Manchester, U.K.

From 1977 to 1992, he was with Federal University of Rio de Janeiro. Since 1993, he has been with the Electrical Engineering Department of Federal University of Juiz de Fora and in 2005 was promoted to Full Professor. His research interests include planning and operation modeling for transmission and distribution systems.

Paulo Augusto Nepomuceno Garcia (M'96) received the B.Sc. degree in 1994 from the Federal University of Juiz de Fora, Juiz de Fora, Brazil, and the M.Sc. and D.Sc. degrees in 1997 and 2001, respectively, from COPPE-Federal University of Rio de Janeiro, Rio de Janeiro, Brazil.

Since 2001, he has been an Associate Professor with the Electrical Engineering Department of Federal University of Juiz de Fora. His main interests are the development of tools for planning and operation of distribution and transmission power systems.